Locating Faults with High Resolution Using Single-Frequency TR-MUSIC Processing

Moussa Kafal, Andrea Cozza, Lionel Pichon

▶ **To cite this version:**

Moussa Kafal, Andrea Cozza, Lionel Pichon. Locating Faults with High Resolution Using Single-Frequency TR-MUSIC Processing. IEEE Transactions on Instrumentation and Measurement, 2016, 65 (10), pp.2342 - 2348. ⟨10.1109/TIM.2016.2578578⟩. ⟨hal-01324059⟩

HAL Id: hal-01324059

https://centralesupelec.hal.science/hal-01324059v1

Submitted on 31 May 2016

HAL is a multi-disciplinary open access archive for the deposit and dissemination of scientific research documents, whether they are published or not. The documents may come from teaching and research institutions in France or abroad, or from public or private research centers.

L'archive ouverte pluridisciplinaire **HAL**, est destinée au dépôt et à la diffusion de documents scientifiques de niveau recherche, publiés ou non, émanant des établissements d'enseignement et de recherche français ou étrangers, des laboratoires publics ou privés.

HAL Authorization

Locating Faults with High Resolution Using Single-Frequency TR-MUSIC Processing

Moussa Kafal, *Student Member, IEEE* Andrea Cozza, *Senior Member, IEEE* and Lionel Pichon

***Abstract*—Time-Reversal multiple signal classification (TR-MUSIC) is here applied to testing cable networks in order to detect and locate soft faults. TR-MUSIC is shown to provide spatial resolution in the millimeter range while using continuous-wave (CW) test signals, even at frequencies with guided wavelengths much larger than cables length. State of the art time-domain reflectometry (TDR) methods would require bandwidths in the order of hundreds of MHz for a similar performance. As opposed to TDR, TR-MUSIC does not suffer from the ambiguity created by the existence of multiple echoes in cable networks, which can be easily misinterpreted as multiple faults, leading to false alarms. TR-MUSIC is intrinsically adapted to dealing with multiple faults, handing a direct estimate of the number of faults found in a network under test. Furthermore, the detection capabilities of TR-MUSIC are insensitive to the severity of a fault, as faults are not detected based on the intensity of their echoes as done in TDR techniques, but on a sub-space approach mostly dependent on phase patterns. Accurate identification of faults from CW signals points to the possibility of designing simpler test systems, not requiring pulse generators and fast electronics. TR-MUSIC accuracy is demonstrated experimentally for locating both single as well as multiple soft faults in two cable networks. The proposed method also gives access to the reflection coefficient of each fault, thus enabling an estimate of its severity.**

***Index Terms*—Fault detection, fault location, soft faults, multiple faults, complex wire networks, TR-MUSIC imaging.**

I. Introduction

Electrical cables are extensively used in nearly all modern systems [1]. They play a primary role in energy and signal distribution where wiring networks are fundamental subsystems whose proper functioning is of critical importance. Eventually, a cable may show signs of weakness which can lead to the appearance of defects and eventually faults. Mainly, wiring faults can be distinguished into two major families: hard faults (open or short circuits), and soft faults (insulation damage, frays, cracks, etc.) [2].

Ensuring the reliable use of cables requires the availability of techniques capable of detecting the presence of faults that could potentially put in jeopardy a whole system [3], [4]. While several electric and non-electric wire diagnosis methods have been studied and developed, reflectometry-based techniques are still in the center stage of research and industrial applications in this domain [5], [6]. Essentially based on a time-domain approach, reflectometry methods inject a test signal into the network under test (NUT) and monitor the reflected one in order to detect the presence, position, and nature of an impedance discontinuity. They have been providing effective results with hard faults due to their high reflection coefficients, but have been showed to be less reliable whenever soft faults are addressed. As a matter of fact, soft faults are usually characterized by weak reflectiveness which produce echoes that can pass unnoticed compared to those caused, e.g., by junctions within an NUT [7], [8], particularly when noisy conditions are present, e.g., in live testing [9]. Add to that, the detection of multiple faults is also mostly limited to hard faults [10].

Moreover, any method based on time-domain analysis, belonging to TDR methods or not, relies on the availability of potentially large bandwidths, in order to create the conditions for spatial resolution. The spatial resolution Δs enabled by a test signal is directly proportional to its spatial support or that of its autocorrelation function, given by

$$\Delta s = k\frac{v}{B_T}, \tag{1}$$

where v is the speed of propagation of electrical signals along the cables of the NUT and B_T is the bandwidth of the test signals; k is a constant of the order of unity, dependent on the shape of the test signals. Limitations are thus introduced by the ability of cables in an NUT to support such bandwidths, as in the case of low-frequency networks such as power grids.

With this background in mind, we studied the possibilities offered by time-reversal (TR) multiple signal classification [11], [12], also known as TR-MUSIC [13]. It has already been applied with success to other detection problems and appears to bring an effective answer to all of the limitations recalled so far [14], [15]. TR-MUSIC is mainly applied for detecting and locating scatterers in a background medium; indeed, soft faults can also be treated as weak scatterers, as argued in [16]. The most striking feature of TR-MUSIC is that it ensures sub-wavelength spatial resolution while working on a single-frequency basis [17], which is in contradiction with (1). Besides, it works independently of *well resolvedness* criteria for multiple scatterers and returns *super-resolution* estimates for their locations. Notably, it is by far less sensitive to scatterer (here fault) coupling [18] which is possible as the TR-MUSIC is based on a sub-space approach.

TR-MUSIC shares the same foundations as DORT-based methods [16], [19], namely, the availability of a mutistatic (or multiport) characterization of the NUT, but they follow two distinguished ways to translate multistatic data into a fault position. DORT-based methods use a sub-space approach in defining signals that, once fed into a numerical model of the NUT, will focus back to the position of a fault; this propagation phase is carried out in the time domain, and therefore undergo

M. Kafal, A. Cozza and L. Pichon are with the Group of Electrical Engineering - Paris (GeePs), CentraleSupelec, Univ. Paris-Sud, Université Paris-Saclay, Sorbonne Universites, UPMC Univ Paris 06, 3 & 11 rue Joliot-Curie, Plateau de Moulon 91192 Gif-sur-Yvette CEDEX, France Contact e-mail: andrea.cozza@ieee.org

most of the same limitations of any other time-domain method, particularly the need for large bandwidth to create spatial resolution. On the contrary, TR-MUSIC, as recalled in Sec. II, does operate on a different sub-space approach, based on the Green function of the NUT; no back-propagation phase is used and actually no test signal is defined. TR-MUSIC operates on phase patterns provided by Green function as a mean of identifying positions in a complex medium.

In this paper, the performance of TR-MUSIC is studied for detecting and locating single as well as multiple soft faults in different network configurations. Experimental results provided at the end of the paper confirm the practical potential of this novel approach. TR-MUSIC is also shown to allow retrieving the reflection coefficient of each fault, thus giving a direct evaluation of the risk they pose to the integrity of the NUT. This step is accomplished without having to measure the reflections of test signals, as no test signal is used in TR-MUSIC.

The structure of this paper is as follows. Section II describes the basic aspects of the TR-MUSIC firstly as initially used in open media for locating scatterers, then as applied to guided-wave propagation along wiring networks for the purpose of soft-fault detection; a procedure for assessing the faults reflection coefficients is then derived. Sec. III presents the results obtained from a thorough measurement campaign, confirming the advantages of TR-MUSIC, in particular millimeter resolutions using low-frequency test signals. The origin behind the appearance of "ghosts" is discussed and shown to be compatible with low-frequency testing.

II. Time-reversal MUSIC

Time reversal was first proposed in acoustics [20], [21]. It has a wide range of applications, including acoustic imaging, nondestructive evaluation, etc. [22], [23]. Over the past decade, there has been an increasing interest in applying TR techniques to electromagnetic waves for imaging purposes in an effort to detect scatterers. TR imaging, DORT, and TR-MUSIC are the three main computational TR methods applied for the sake of target detection [17], [24]. TR imaging is intrinsically a time-domain method that can be applied only to scenarios where a source is identified by tracing back in time the field it has radiated. DORT extends this concept to the case of scatterers, acting as secondary sources of radiation. The application of DORT to fault detection was introduced in [16], [19], proving it has advantages with respect to standard TDR techniques. Yet, it is also a time-domain method, where spatial resolution can only be gained by means of pulsed signals, i.e., large bandwidths.

In our case study we will focus on TR-MUSIC, as it has presented major advantages over the remaining methods, in particular super-resolution while using single-frequency data. As we work exclusively in the frequency domain, from this point onward we will not explicitly display the frequency variable.

A. Standard definition for open media

In TR imaging a generic position X_p in a medium is probed for targets by means of a quantity, such as a field or a voltage, generated by a set of N transceivers; their interdependence can be modeled as a vector Green function $\boldsymbol{g}(X_p)$. The transceivers also sample the backscattered fields (or voltages), yielding a scattering matrix $\boldsymbol{S}$ of dimensions $N \times N$. This scattering matrix is then used to compute the TR operator (TRO) $\boldsymbol{K} = \boldsymbol{S}^H \boldsymbol{S}$, where the superscript H is the Hermitian transpose. TR-MUSIC was shown to be capable of locating M point targets from the knowledge of the TRO under the condition that $N > M$ [12], [17]. It does so by computing the eigenvalue decomposition of $\boldsymbol{K}$, which is also equivalent to the singular value decomposition of $\boldsymbol{S}$ [25]

$$\boldsymbol{K} = \boldsymbol{U}\boldsymbol{\Lambda}\boldsymbol{U}^H, \tag{2}$$

where $\boldsymbol{\Lambda}$ is a real-valued diagonal matrix containing the eigenvalues, and $\boldsymbol{U}$ is the eigenvector matrix. In fact, $\boldsymbol{U}$ can be divided into a signal space $\mathcal{S}$ and a noise space $\mathcal{N}$; the latter can be seen as an approximation of the null space of $\boldsymbol{K}$. $\mathcal{S}$ is identified by the eigenvectors associated with the most significant eigenvalues, with respect to a threshold λ_{th}, i.e., $\mathcal{S} = \mathrm{span}\{\boldsymbol{u}_i : \lambda_i > \lambda_{th}\}$, whereas $\mathcal{N}$ is formed by the remaining eigenvectors deemed to have negligible eigenvalues $\mathcal{N} = \mathrm{span}\{\boldsymbol{u}_i : \lambda_i < \lambda_{th}\}$, with λ_i and $\boldsymbol{u}_i$ are the eigenvalues and their corresponding eigenvectors, respectively; λ_{th} is set by analyzing the scree plot of the eigenvalues of $\boldsymbol{K}$.

TR-MUSIC works by computing for each position X_p in the medium the quantity

$$\Phi(X_p) = \frac{1}{\sum_i \left|\boldsymbol{u}_i^H \boldsymbol{g}(X_p)\right|^2}, \tag{3}$$

where the sum is taken only over the $N-M$ indexes i such that $\lambda_i < \lambda_{th}$; $\Phi(X_p)$ is usually referred to as pseudo-spectrum [11]. In fact, the inner product $\boldsymbol{u}_i^H \boldsymbol{g}(X_p)$ will vanish whenever a test location X_p happens to correspond to the actual position of one of the targets, since the significant eigenvectors of the TRO were demonstrated to be a linear combinations of the medium Green function sampled at the targets position [12], [24]; consequently, the pseudo-spectrum $\Phi(X_p)$ is singular at each scatterer position. More importantly, $\Phi(X_p)$ computed at any single frequency is capable of pointing the locations of the scatterers. Accordingly, TR-MUSIC does not require a large bandwidth to provide good spatial resolution, in contrast to time-domain fault-detection methods [3], [7], [8].

B. Application to wiring networks

Since a fault in an NUT is fundamentally an impedance discontinuity, it behaves as a lumped scatterer. This observation implies that identifying the position of a fault is basically the same problem as locating a scatterer in a generic medium. As such, TR-MUSIC applied to fault detection is based on the availability of the NUT's scattering matrix, which can be measured, as discussed in sec. III-A, by means of a vector network analyzer (VNA).

As it is typically the case when dealing with soft faults, applying the baselining approach, i.e., taking the difference between the response of the NUT, containing an eventual fault, and a reference response of a healthy (reference) version is an

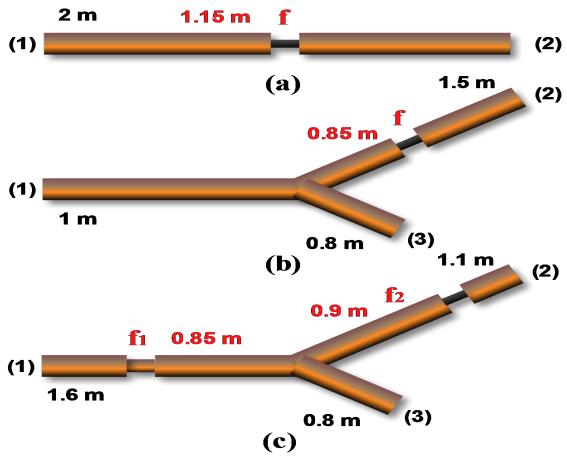

Fig. 1: Layouts of the NUTs considered in the experimental validation of the TR-MUSIC: (a) single-branch NUT with a single soft fault; (b) single-junction network configuration having a single soft fault; and (c) single-junction NUT having two different severity soft faults. All structures include the length of the cables as well as the position of the faults (position of the second fault is measured from the junction).

effective solution to remove the spurious echoes generated by impedance discontinuities like junctions, leaving only those echoes initially generated by the interaction between the testing signals and the faults [2], [26]. Furthermore, removing the echoes generated by junctions is also beneficial in order to increase the maximum number of faults M that TR-MUSIC can detect, which is limited to $N-1$.

Consequently, baselining ideally leaves a scattering matrix with nothing else than the signature of the faults. Accordingly, the NUT's response after baselining will be $\boldsymbol{S} = \boldsymbol{S}_f - \boldsymbol{S}_h$, with $\boldsymbol{S}_f$ and $\boldsymbol{S}_h$ the scattering matrices of the (eventually) faulty NUT and its healthy (reference) version, respectively. This matrix is then processed as described in the previous section.

The pseudo-spectrum (3) requires an a priori model the Green function of the medium, as also required in any approach to time-reversal imaging. In the case of a wiring network, the reference model is computed by means of a numerical simulator for transmission lines, modeling the layout of the healthy NUT, which needs to be known. The Green function here relates the voltage at a position along the healthy NUT with the N excitation voltages applied to its test ports.

C. Estimating a fault severity

Once the position of each fault in the NUT are found thanks to the pseudo spectrum (3), it is possible to estimate the NUT response $\boldsymbol{S}_i$ that would be measured if only one fault at a time appeared. As discussed in [19], as long as soft faults are considered, the first Born approximation holds, thus the global scattering matrix of any faulty NUT can be broken down as

$$\boldsymbol{S}_G \approx \sum_{i=1}^{M} \boldsymbol{S}_i. \tag{4}$$

Fig. 2: The two faulty samples used to introduce soft faults within the NUTs for the experimental tests where the increasing the crushed area intensifies the reflection coefficient of the fault.

The main limitation in (4) is its neglecting interactions between multiple faults [19], which can induce errors, as discussed in sec. III-C.

Now the problem is that the fault reflection coefficients $\{\Gamma_i\}$ are unknown. As long as the faults are soft, i.e., $|\Gamma_i| \ll 1, \forall i$,the propagation of voltage waves within the NUT would be hardly affected, again under Born first approximation. This observation implies that a dummy fault of known value $\Gamma_{d,i}$ can be used instead of the real unknown fault Γ_i, yielding a scattering matrix $\boldsymbol{S}_{d,i}$. This latter is ideally identical to $\boldsymbol{S}_i$, but for the factor $\Gamma_i/\Gamma_{d,i}$. Introducing the matrices $\tilde{\boldsymbol{S}}_i = \boldsymbol{S}_{d,i}/\Gamma_{d,i}$, the $\{\Gamma_i\}$ can be estimated by solving the least-square problem

$$\min_{\{\Gamma_i\}} \left\| \boldsymbol{S}_G - \sum_{i=1}^{M} \Gamma_i \tilde{\boldsymbol{S}}_i \right\|^2, \tag{5}$$

i.e., by using the $\{\tilde{\boldsymbol{S}}_i\}$ as regressors for the measured scattering matrix $\boldsymbol{S}$.

III. Results and Analysis

The performance of TR-MUSIC as presented in sec. II-B was tested against experimental data measured from NUTs affected by a single as well as multiple soft faults. As explained in sec. II-C, having extracted the position of the faults, their reflection coefficients can also be estimated, as tested in the last part of this section.

A. Experimental setup

Two NUTs with different complexity are considered, for three fault configurations: a single-branch single-fault (SB-SF), a single-junction single-fault (SJ-SF) and a single-junction double-fault (SJ-DF) configuration, presented in Fig. 1.

The NUTs are implemented using standard 50 Ω coaxial cables as transmission lines. A set of 30-cm long samples made of semi-rigid coaxial lines of 3.4 mm cross-section, as those shown in Fig. 2, were used in order to introduced faults. This approach offers a sizable advantage, since faults

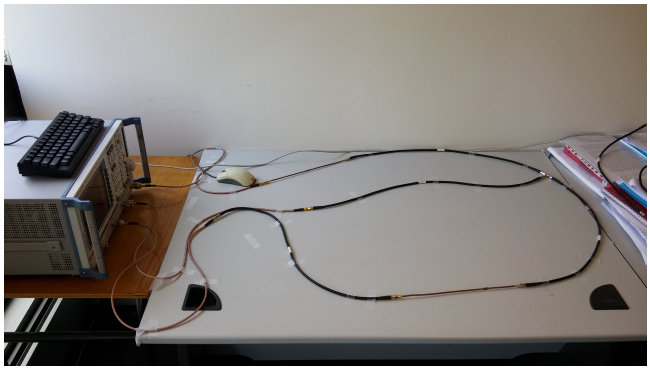

Fig. 3: Experimental setup for the single-junction NUT, containing two faulty sections, connected to the VNA for the experimental tests, schematized in Fig. 1(c).

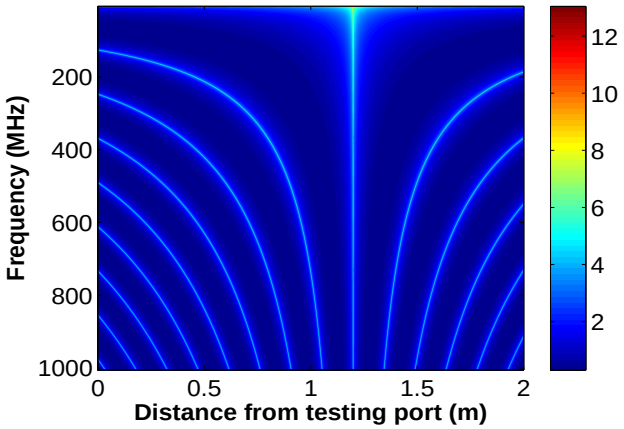

Fig. 4: Pseudo-spectrum of the TR-MUSIC applied on the SB-SF NUT of Fig. 1(a) on a frequency range from 1 MHz to 1 GHz.

can be introduced and removed in a controllable manner, rather than directly, and irreversibly, by damaging a cable. Soft faults were created by applying a crushing force to the samples, thus reducing their cross-section to 2 mm, over a different portion of length, producing faults of varying severity: the strongest soft fault was designated by a crushed area of 2 cm while the weaker one by 1 cm; undamaged samples were also available, serving as a reference for the healthy version of the NUT. This same approach has already been used in [16], [19], where it allowed a practical and reproducible framework. The faults severity were shown in [19] to be $\Gamma_{f1} \simeq 2.7\Gamma_{f2}$, with Γ_{f1} and Γ_{f2} being the reflection coefficients of the stronger and the weaker faults, respectively.

The ends of the cables making up each NUT were used as testing ports, by connecting them to a Rohde & Schwarz ZVB8 VNA, covering a frequency range from 300 kHz to 8 GHz, with four testing ports; an example of complete setup is shown in Fig. 3. The measurement of the scattering matrices was done over different bandwidths and frequency steps depending on the configuration of the NUT, lengths of the cables and the desired testing conditions, as will be detailed later on. After calibrating the VNA using the calibration kit provided by the manufacturer, studying the network consisted of two steps: 1) measurement of $\boldsymbol{S}_h$ of the reference healthy system with the unaltered 30-cm semi-rigid sections; 2) measurement of $\boldsymbol{S}_f$ of the NUT, after replacing the reference samples with the crushed ones.

Henceforth, the procedure described in sec. II-B is applied. Consequently, in order to compute the pseudo spectrum of each NUT, the Green functions of their healthy version are computed by means of an in-house transmission-line solver, implemented under Matlab.

B. Experimental validation

The proposed method was first applied to the SB-SF NUT in Fig. 1(a). The corresponding scattering matrices were measured in the frequency domain using the VNA, covering the frequency range from 1 MHz to 1 GHz, with 1 MHz steps.

Fig. 4 shows the pseudo-spectrum computed from experimental data; the distances on the horizontal axis are measured from port no.1, as defined in Fig. 1. Several features need to be commented. First, a number of singularities appear at each frequency, but only one keeps constant, at a position corresponding to the fault, at 1.15 m, with an standard deviation through the entire set of frequencies well below the millimeter. This observation confirms the claims of the possibility of locating very accurately a fault while working at a single frequency, as opposed to time-domain methods.

The remaining singularities are reminiscent of ghosts found in radar applications in multi-path media. The fact that their position changes with the frequency and that for a given frequency they are periodically spaced is a direct indication of their origin. In fact, these ghosts can be understood by recalling the periodicity of wave propagation of harmonic signals, proper to single-branch structures; indeed, the spatial period corresponds to half a wavelength at each frequency tested. In other words, the periodicity of the Green function along a cable imply that the pseudo-spectrum will also be periodic, but it will change with the frequency.

Ghosts are confusing and cannot be distinguished from the actual position of a fault, when observed at a single frequency. Therefore they need to be avoided by ensuring that for a maximal length L found through an NUT, the test frequency is $f \lesssim v/(2L)$,with v being the speed of the wave along the NUT.

Setting a maximum frequency equal to 100 MHz, TR-MUSIC was applied to the three NUTs in Fig. 1, obtaining the pseudo-spectra shown in Fig. 5. All of them present only a singularity at the fault position. Of notable interest is the last case, featuring two faults, where both of them are characterized by a sub-millimeter accuracy, as computed across all the frequencies tested. Passing from one to two faults does not modify in any aspect the interpretation of the pseudo-spectra, proving the robustness of TR-MUSIC to multiple-scatterer configurations. This seamless passage from single to multiple faults is in sharp contrast with the efforts reported in the literature for TDR techniques, where multiple faults can lead to ambiguity in their localization, particularly when

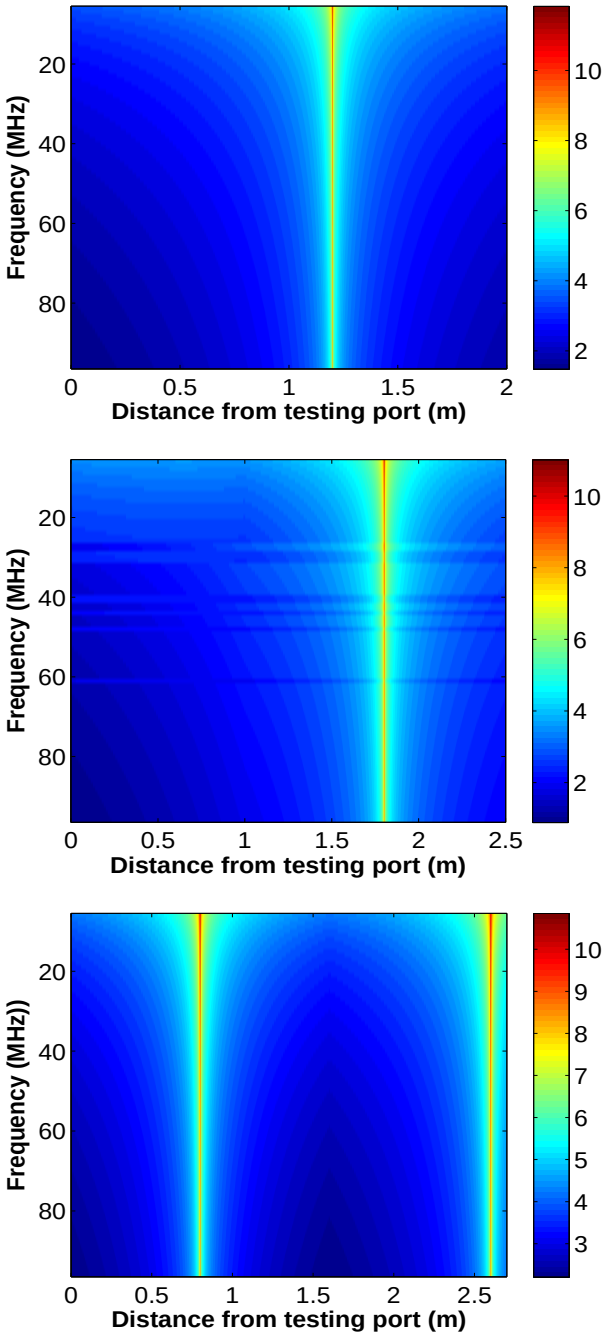

Fig. 5: Pseudo-spectra computed for the three NUTs in Fig. 1, on a frequency range from 1 MHz to 100 MHz.

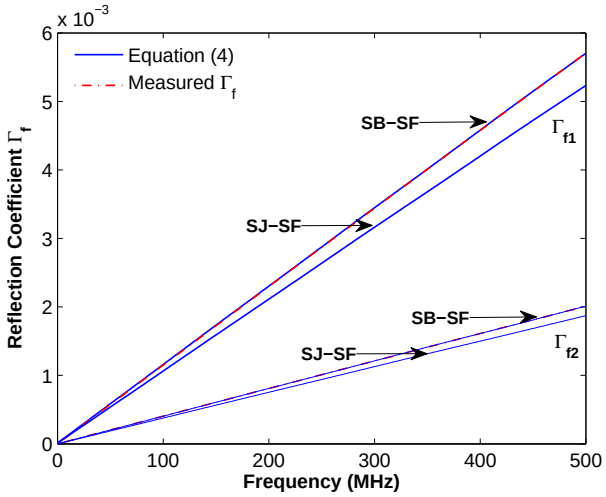

Fig. 6: Amplitude of the measured reflection coefficient of the stronger as well as the weaker faulty sections of Fig. 2 versus the frequency used in the experimental validation of the SB-SF and SJ-SF NUTs. Estimates are obtained by means of (5) applied on the experimental data and direct measurements from the VNA.

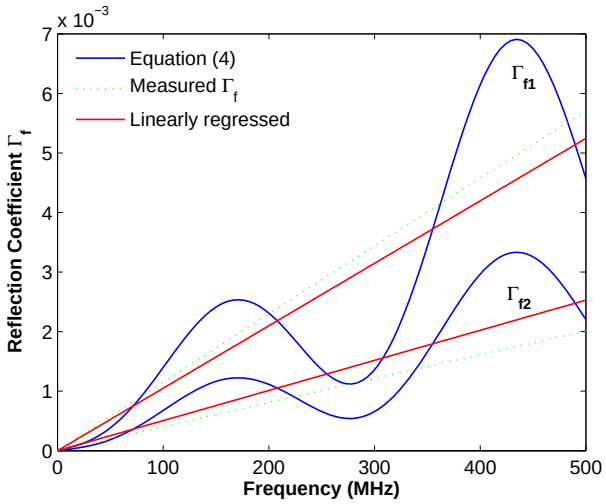

Fig. 7: The reflection coefficients of the two faulty sections used in the experimental setup of Fig. 3. The results are estimated by means of (5) with an application of a linear regression as discussed in the body of the text along with direct VNA measurements.

dealing with complex NUTs.

C. Retrieving a fault's reflection coefficient

Having inferred the position of the faults in each of the three NUTs, the reflection-coefficient estimation technique presented in sec. II-C was then applied for each frequency tested. The longer and stronger fault in Fig. 2 is first considered, as found in the experimental setups of Fig. 1 (a)-(b); along with similar experimental measurements done on the same configurations but with the shorter weak fault where the results obtained are shown in Fig. 6. The estimate provided by (5) closely agrees with the measured reflection coefficients for the SB-SF and SJ-SF configurations. The worst estimate error is 8.5% when considering the SJ-SF case (a maximum of 8.3% for the stronger and 6.8% for the weaker).

The same operations were applied to the SJ-DF NUT, in order to assess the accuracy of the estimation for both faults in multiple faulty complex networks. Fig. 7 shows the reflection coefficients of the two faulty samples as obtained from the measured and the (5)-based estimates whose values appear

to oscillate around the true values. In fact, this behavior is likely caused by the interactions between the two faults and also with the junction, and was also observed in [19], when attempting to estimate fault severity using a eigenvector-based projection approach. The systematic error introduction by the interactions represents a problem when testing an NUT with a single frequency, since the estimate can locally deviate rather strongly. Interestingly, interactions have an impact only on the estimate of the faults severity, not on their positions.

On the other hand, repeating tests at multiple frequencies and applying a simple linear regression, the intensity of these oscillations can be reduced, as shown in Fig. 7 where one fifth of the frequency points were used for this sake (100 out of 500 samples). This need for multiple-frequency regression could clearly be avoided by looking for the entire set of reflection coefficients at once, rather than separating the system into single-fault contributions, as done in Sec. II-C. The price to pay would be a non-linear optimization process, which is out of the scope of this paper. Nonetheless, the estimates obtained are rather precise. More importantly, they are not based on any measure of the intensity of signals reflected by faults, but are rather entirely based on sub-space computations, which are intrinsically more robust to noise and multiple reflections observed in complex NUTs.

IV. Conclusions

This paper has investigated the potential of TR-MUSIC as a single-frequency fault detection technique. Experiments have shown that this technique is effective in detecting and locating single as well as multiple soft faults in two NUTs of different complexity. Of practical importance is its ability to retrieve a fault's reflection coefficient even though a reflectogram is not defined.

The appearance of ghosts in pseudo-spectra was shown to be avoidable by imposing a maximum test frequency, according to the length of the NUT. The surprising ability of TR-MUSIC to ensure a sub-millimeter resolution while using relatively low test frequencies is good news, as similar performance with TDR techniques would require much higher test frequencies and wider bandwidths, which may be hampered by attenuation in cables. Furthermore, since this paper has shown that the performance of TR-MUSIC does not depend on the chosen test frequency, TR-MUSIC appears as more readily adaptable to the case of live testing, where the NUT would be under use over a given set of frequencies and thus test signals could ideally be allocated outside these frequencies. The same rationale clearly applies to EMC constraints.

Future work will need to deal with the robustness of the TR-MUSIC and its sensitivity to the presence of noise.

References

[1] C. Furse and R. Haupt, "Down to the wire [aircraft wiring]," *Spectrum, IEEE*, vol. 38, no. 2, pp. 34–39, 2001.

[2] L. A. Griffiths, R. Parakh, C. Furse, and B. Baker, "The invisible fray: A critical analysis of the use of reflectometry for fray location," *Sensors Journal, IEEE*, vol. 6, no. 3, pp. 697–706, 2006.

[3] F. Auzanneau, "Wire troubleshooting and diagnosis: Review and perspectives," *Progress In Electromagnetics Research B*, vol. 49, pp. 253–279, 2013.

[4] Y.-J. Shin, E. J. Powers, T.-S. Choe, C.-Y. Hong, E.-S. Song, J.-G. Yook, and J. B. Park, "Application of time-frequency domain reflectometry for detection and localization of a fault on a coaxial cable," *Instrumentation and Measurement, IEEE Transactions on*, vol. 54, no. 6, pp. 2493–2500, 2005.

[5] C. P. Nemarich, "Time domain reflectometry liquid level sensors," *Instrumentation & Measurement Magazine, IEEE*, vol. 4, no. 4, pp. 40–44, 2001.

[6] N. Paulter, "An assessment on the accuracy of time-domain reflectometry for measuring the characteristic impedance of transmission lines," *Instrumentation and Measurement, IEEE Transactions on*, vol. 50, no. 5, pp. 1381–1388, 2001.

[7] S. J. P., *Time-domain Reflectometry for Monitoring Cable Changes: Feasibility Study*. Electric Power Research Institute, 1990.

[8] C. Furse, Y. C. Chung, R. Dangol, M. Nielsen, G. Mabey, and R. Woodward, "Frequency-domain reflectometry for on-board testing of aging aircraft wiring," *Electromagnetic Compatibility, IEEE Transactions on*, vol. 45, no. 2, pp. 306–315, 2003.

[9] Q. Zhang, M. Sorine, and M. Admane, "Inverse scattering for soft fault diagnosis in electric transmission lines," *Antennas and Propagation, IEEE Transactions on*, vol. 59, no. 1, pp. 141–148, 2011.

[10] H. Boudjefdjouf, R. Mehasni, A. Orlandi, H. Bouchekara, F. De Paulis, and M. Smail, "Diagnosis of multiple wiring faults using time-domain reflectometry and teaching–learning-based optimization," *Electromagnetics*, vol. 35, no. 1, pp. 10–24, 2015.

[11] R. O. Schmidt, "Multiple emitter location and signal parameter estimation," *Antennas and Propagation, IEEE Transactions on*, vol. 34, no. 3, pp. 276–280, 1986.

[12] H. Lev-Ari and A. Devancy, "The time-reversal technique re-interpreted: Subspace-based signal processing for multi-static target location," in *Sensor Array and Multichannel Signal Processing Workshop. 2000. Proceedings of the 2000 IEEE*. IEEE, 2000, pp. 509–513.

[13] A. J. Devaney, E. A. Marengo, and F. K. Gruber, "Time-reversal-based imaging and inverse scattering of multiply scattering point targets," *The Journal of the Acoustical Society of America*, vol. 118, no. 5, pp. 3129–3138, 2005.

[14] M. E. Yavuz and F. L. Teixeira, "Ultrawideband microwave sensing and imaging using time-reversal techniques: A review," *Remote Sensing*, vol. 1, no. 3, pp. 466–495, 2009.

[15] D. Ciuonzo, G. Romano, and R. Solimene, "Performance analysis of time-reversal music," *Signal Processing, IEEE Transactions on*, vol. 63, no. 10, pp. 2650–2662, 2015.

[16] L. Abboud, A. Cozza, and L. Pichon, "A noniterative method for locating soft faults in complex wire networks," *Vehicular Technology, IEEE Transactions on*, vol. 62, no. 3, pp. 1010–1019, 2013.

[17] A. J. Devaney, "Super-resolution processing of multi-static data using time reversal and music," *J. Acoust. Soc. Am*, 2000.

[18] F. K. Gruber, E. A. Marengo, and A. J. Devaney, "Time-reversal imaging with multiple signal classification considering multiple scattering between the targets," *The Journal of the Acoustical Society of America*, vol. 115, no. 6, pp. 3042–3047, 2004.

[19] M. Kafal, A. Cozza, and L. Pichon, "Locating multiple soft faults in wire networks using an alternative dort implementation," *Instrumentation and Measurement, IEEE Transactions on*, vol. 65, no. 2, pp. 399–406, 2016.

[20] M. Fink *et al.*, "Time-reversed acoustics," *Scientific American*, vol. 281, no. 5, pp. 91–97, 1999.

[21] M. Fink and C. Prada, "Acoustic time-reversal mirrors," *Inverse problems*, vol. 17, no. 1, p. R1, 2001.

[22] Y. Hristova, P. Kuchment, and L. Nguyen, "Reconstruction and time reversal in thermoacoustic tomography in acoustically homogeneous and inhomogeneous media," *Inverse Problems*, vol. 24, no. 5, p. 055006, 2008.

[23] W. Zhang, A. Hoorfar, and L. Li, "Through-the-wall target localization with time reversal music method," *Progress In Electromagnetics Research*, vol. 106, pp. 75–89, 2010.

[24] C. Prada and M. Fink, "Eigenmodes of the time reversal operator: A solution to selective focusing in multiple-target media," *Wave motion*, vol. 20, no. 2, pp. 151–163, 1994.

[25] W. GAO, X. WANG, and B. Wang, "Review of time reversal imaging techniques."

[26] G. Cerri, R. De Leo, L. Della Nebbia, S. Pennesi, V. M. Primiani, and P. Russo, "Fault location on shielded cables: Electromagnetic modelling and improved measurement data processing," *IEE Proceedings-Science, Measurement and Technology*, vol. 152, no. 5, pp. 217–226, 2005.